Long-lived qubit memory using atomic ions

C. Langer,* R. Ozeri, J. D. Jost, J. Chiaverini, B. DeMarco,† A. Ben-Kish,‡ R. B. Blakestad, J. Britton, D. B. Hume, W. M. Itano, D. Leibfried, R. Reichle, T. Rosenband, T. Schaetz,§ P. O. Schmidt,¶ and D. J. Wineland
National Institute of Standards and Technology, 325 Broadway, Boulder, Colorado 80305, USA
(Dated: April 10, 2005)

We demonstrate experimentally a robust quantum memory using a magnetic-field-independent hyperfine transition in $^9Be^+$ atomic ion qubits at a magnetic field $B \simeq 0.01194$ T. We observe that the single physical qubit memory coherence time is greater than 10 seconds, an improvement of approximately five orders of magnitude from previous experiments with $^9Be^+$. We also observe long coherence times of decoherence-free subspace logical qubits comprising two entangled physical qubits and discuss the merits of each type of qubit.

PACS numbers: 03.67.Pp, 32.60.+i, 03.65.Yz, 03.67.Mn

Scalable quantum information processing (QIP) requires physical systems capable of reliably storing coherent superpositions for periods over which quantum error correction can be implemented [1]. Moreover, suppressing memory error rates to very low levels allows for simpler error-correcting algorithms [2, 3]. In many current atomic ion QIP experiments, a dominant source of memory error is decoherence induced by fluctuating ambient magnetic fields [4, 5]. To address this problem, we investigate creating long-lived qubit memories using a first-order magnetic-field-independent hyperfine transition and logical qubits of a decoherence-free subspace [6].

Atomic systems have proven themselves as good candidates for quantum information storage through their use in highly stable atomic clocks [7]. Here, the principle of using first-order magnetic-field-independent transitions is well established. A typical clock transition $|F, m_F = 0\rangle \leftrightarrow |F', m_{F'} = 0\rangle$ between hyperfine states of angular momentum F and F' in alkali atoms has no linear Zeeman shift at zero magnetic field, and coherence times exceeding 10 minutes have been observed [8]. Unfortunately, magnetic sublevels in each hyperfine manifold are degenerate at zero magnetic field. This makes it more advantageous to operate at a nonzero field in order to spectrally resolve the levels, thereby inducing a linear field dependence of the transition frequency. However, field-independent transitions between hyperfine states also exist at nonzero magnetic field. In the context of atomic clocks, coherence times exceeding 10 minutes have been observed in $^9Be^+$ ions at a magnetic field $B = 0.8194$ T [9].

In neutral-atom systems suitable for QIP, field-independent transitions at nonzero magnetic field have been investigated in rubidium [10, 11]. The radio-frequency (RF)/microwave two-photon stimulated-Raman hyperfine transition $|F = 1, m_F = -1\rangle \leftrightarrow |F' = 2, m_{F'} = 1\rangle$ is field-independent at approximately 3.23×10^{-4} T , and coherence times of 2.8 s have been observed [11]. In these and the clock experiments, transitions were driven by microwave fields on large numbers of atoms. Using microwaves, it may be difficult to localize the fields well enough to drive individual qubits unless a means (e.g., a magnetic-field gradient or Stark-shift gradient) is employed to provide spectral selection [12, 13], a technique that has the additional overhead of keeping track of the phases induced by these shifts. With transitions induced by laser beams, the addressing can be accomplished by strong focusing [5] or by weaker focusing and inducing transitions in separate trap zones [4]. In contrast to microwave fields, optical fields (using appropriate geometry [14, 15]) provide stronger field gradients that are desirable for coupling ion motional states with internal states, a requirement for certain universal multi-qubit logic gates [14, 16]. Here, we explore the coherence time of a single atomic ion qubit in a scalable QIP architecture using laser beam addressing.

In recent $^9Be^+$ QIP experiments utilizing 2s $^2S_{1/2}$ hyperfine states: $|F = 2, m_F = -2\rangle$ and $|F = 1, m_F = -1\rangle$ as qubit levels, fluctuating ambient magnetic fields caused significant decoherence [4, 17]. There, the qubit transition depended linearly on the magnetic field with a coefficient of approximately 21 kHz/μT (Fig. 1). Thus, random magnetic field changes of 0.1 μT (typical in our laboratories) would dephase qubit superpositions (to a phase uncertainty of 1 rad) in 80 μs. To mitigate this decoherence, refocussing spin-echo π-pulses were inserted in the experimental sequences [4, 17] to limit the bandwidth of noise to which the qubits were susceptible. However, these effects could not be eliminated completely, and fluctuating fields remained a major source of error in these experiments.

The energy spectrum of the ground hyperfine states of $^9Be^+$ as a function of magnetic field is shown in Fig. 1. At $B_0 \simeq 0.01194$ T, the transition $|F = 2, m_F = 0\rangle \equiv |\downarrow\rangle \leftrightarrow |F = 1, m_F = 1\rangle \equiv |\uparrow\rangle$ (frequency $\nu_{\uparrow\downarrow} \simeq 1.2$ GHz) is first-order field-independent with second-order dependence given by $(0.305\ \mathrm{Hz}/\mu\mathrm{T}^2)(B - B_0)^2$. Given random magnetic field changes of 0.1 μT, we expect superpositions of $|\downarrow\rangle$ and $|\uparrow\rangle$ to dephase in approximately 50 s. The transition $|F = 2, m_F = 2\rangle \equiv |A\rangle \leftrightarrow |\uparrow\rangle$ (frequency $\nu_{\uparrow A} \simeq 1.0$ GHz) is first-order field sensitive with linear dependence of 17.6 kHz/μT for $B = B_0$. We use frequency

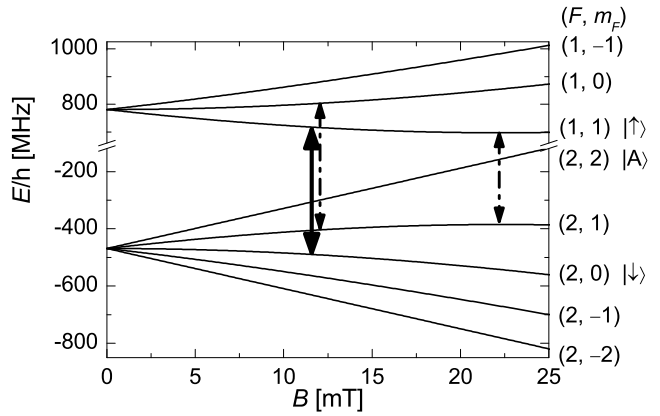

FIG. 1: Hyperfine level structure of the $2s\ ^2S_{1/2}$ state of $^9Be^+$. The solid arrow indicates the magnetic-field-independent transition studied here (0.01194 T); the dashed arrows indicate other useful field-independent transitions at 0.01196 T and 0.02231 T.

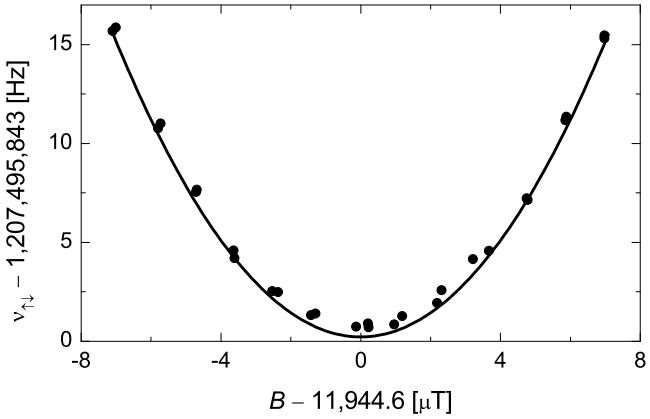

FIG. 2: Frequency of the field-independent transition $|\downarrow\rangle \leftrightarrow |\uparrow\rangle$ as a function of magnetic field. Circles are measured data points; the solid curve is a theoretical prediction. The statistical uncertainty of each datum is $\Delta B \lesssim 3$ nT and $\Delta\nu_{\uparrow\downarrow} \lesssim 0.3$ Hz.

measurements of this transition as a probe of the magnetic field. We note that the $|F = 2, m_F = 1\rangle \leftrightarrow |F' = 1, m_{F'} = -1\rangle$ transition, similar to that in Rb [10, 11], is field-independent in $^9Be^+$ at $B = 2.54 \times 10^{-5}$ T; however, using detuned laser excitation fields, this transition is less practical as it is a four-photon transition.

In the experiment, a single $^9Be^+$ ion is confined to a zone of a trap similar to that in Ref. [18]. The ion is optically pumped to the state $|A\rangle$, and its motion is Doppler cooled by use of the cycling transition $|A\rangle \leftrightarrow |2p\ ^2P_{3/2}, F' = 3, m_{F'} = 3\rangle$ [15]. We detect the state of the $^9Be^+$ ion through state-dependent resonance fluorescence [15]. That is, with light tuned to the cycling transition, the state $|A\rangle$ fluoresces strongly, whereas the other states do not. Using coherent rotations described below, we measure the $|\downarrow\rangle$, $|\uparrow\rangle$ "qubit" level populations by mapping the states $|\uparrow\rangle$ and $|\downarrow\rangle$ to $|A\rangle$ and $|\uparrow\rangle$ respectively and measuring the state $|A\rangle$.

Coherent rotations between states $|A\rangle \leftrightarrow |\uparrow\rangle$ and $|\uparrow\rangle \leftrightarrow |\downarrow\rangle$ have the form (in the Bloch sphere representation)

$$R(\theta, \phi) = \cos\frac{\theta}{2}\, I - i \sin\frac{\theta}{2} \cos\phi\ \sigma_x - i \sin\frac{\theta}{2} \sin\phi\ \sigma_y, \quad (1)$$

where I is the identity matrix, σ_i are Pauli operators, θ is the rotation angle, and ϕ is the angle from the x-axis to the rotation axis (in the x-y plane). These rotations are driven by two-photon stimulated Raman transitions using focused laser beams [15, 16]. We modulate one polarization component of a single laser beam with an electro-optic modulator. This technique simplifies the stabilization of differential optical path length fluctuations between the two Raman beams (generated by the two polarizations), similar to Ref. [19]. The difference in optical path is due solely to the static birefringence of the modulator's electro-optic crystal. We stabilize fluctuations in the birefringence by measuring the retardation with an optical phase detector similar to that in Ref. [20] and feeding back on the temperature of an additional birefringent crystal in the beam path. Small offsets of the retardation from its optimal value of $\lambda/4$ only reduce the magnitude of the Rabi frequency to second order and do not alter the phase of subsequent rotations.

To characterize the field-independent transition, we perform Ramsey spectroscopy [21] on the two transitions $|A\rangle \leftrightarrow |\uparrow\rangle$ and $|\downarrow\rangle \leftrightarrow |\uparrow\rangle$ for different magnetic fields (Fig. 2). The magnetic field is determined from the $\nu_{\uparrow A}$ measurement. By measuring $\nu_{\uparrow\downarrow}$ at $B = B_0$ for different RF trapping strengths and extrapolating to zero, we can determine the corresponding AC Zeeman shift produced by the trap's RF currents. This shift [1.81(2) Hz] was removed from the data in Fig. 2. The calculated solid curve in Fig. 2 is derived from data in Refs. [9, 22].

We measure the qubit coherence time by tuning the magnetic field to the minimum of Fig. 2 and performing Ramsey spectroscopy on the $|\downarrow\rangle \leftrightarrow |\uparrow\rangle$ transition for different Ramsey intervals T_R. The $^9Be^+$ ion is first Doppler cooled and prepared in the state $|\uparrow\rangle$. We then apply the rotation $R(\frac{\pi}{2}, 0)$, creating the superposition state $|\Psi_1\rangle = \frac{1}{\sqrt{2}}(|\uparrow\rangle - i|\downarrow\rangle)$ and wait for the Ramsey interval T_R during which the state evolves to $|\Psi_2\rangle = \frac{1}{\sqrt{2}}(e^{i\phi_D}|\uparrow\rangle - i|\downarrow\rangle)$. The phase ϕ_D is given by the integrated detuning of the local oscillator frequency (which modulates the Raman laser frequency) with respect to the qubit transition frequency over the Ramsey interval T_R. A second rotation $R(\frac{\pi}{2}, \phi)$ is then applied to our qubit with ϕ variable. Repeating the experiment many times and performing a projective

measurement of the state $|\uparrow\rangle$ as described above yields

$$P_\uparrow = \frac{1}{2}(1 - \cos(\phi_D + \phi)), \tag{2}$$

the probability of measuring the state $|\uparrow\rangle$. The measurement sequence is repeated for different phases ϕ, and the detected probability $P_\uparrow$ is fit to the function $f = a - \frac{b}{2}\cos(d\phi + \phi_D)$. The fit parameter d allows for magnetic-field drift in time as successive phase points are recorded sequentially; d is close to unity for all scans in this data set. Phase scans for $T_R = 4$ ms and 4 s are shown in Fig. 3a. Any phase fluctuation of the qubit state with respect to our local oscillator (derived from a Hydrogen maser source with negligible phase uncertainty compared to that of the qubit state) during the Ramsey interval T_R will reduce the contrast b. The contrast b for different T_R is fit to the exponential $b(T_R) = b_0 e^{-T_R/\tau}$ (Fig. 3b). We find the coherence time for our field-independent qubit to be $\tau = 14.7 \pm 1.6$ s. The qubit coherence time is limited by slow drift of the magnetic field over the measurement time scale of a single point. For the $T_R = 4$ s data in Fig. 3a, this time scale is 400 s. In principle, if the magnetic-field drift is small for the period of a single measurement, we can interrupt data collection to measure (via $\nu_{\uparrow A}$) and correct for magnetic-field deviations from B_0.

Logical qubits of the decoherence-free subspace (DFS) [6] comprising two entangled physical qubits in the form of Bell states,

$$|\Psi_\pm\rangle = \frac{1}{\sqrt{2}}(|01\rangle \pm |10\rangle), \tag{3}$$

are also immune to fluctuations in magnetic fields. Any phase acquired due to a (uniform) fluctuation of magnetic field by one state of the superposition is acquired equally by the other state of the superposition. In the experiment described below (performed in a separate but similar trap), the physical qubit states $|0\rangle$ and $|1\rangle$ are the magnetic-field-sensitive hyperfine states $|F = 1, m_F = -1\rangle$ and $|F = 2, m_F = -2\rangle$ respectively at a field $B \simeq 0.0013$ T. Using the technique of Ref. [23] as described below, we demonstrate that entanglement is long-lived.

Even though the states $|\Psi_\pm\rangle$ are immune to uniform time-varying magnetic fields, they are *not* protected from noise in a magnetic-field difference between the locations of the two ions. Such a gradient can cause the states $|01\rangle$ and $|10\rangle$ to acquire phase at a differential rate $\Delta\phi(t)$ due to the different local magnetic fields. This results in a coherent oscillation between $|\Psi_+\rangle$ and $|\Psi_-\rangle$ according to

$$|\psi(t)\rangle = \cos\Big[\frac{\Delta\phi(t)}{2}\Big]|\Psi_+\rangle + i\sin\Big[\frac{\Delta\phi(t)}{2}\Big]|\Psi_-\rangle. \tag{4}$$

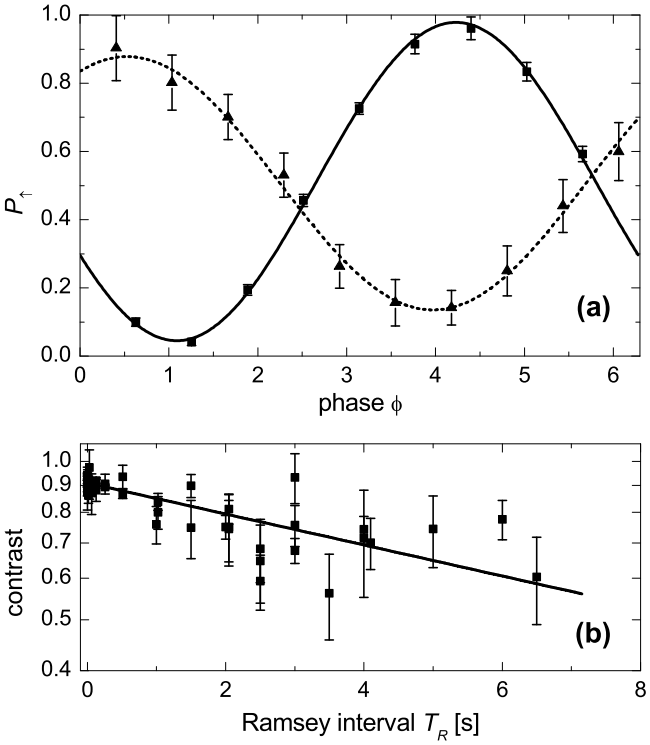

FIG. 3: **(a)** Ramsey data at $T_R = 4$ ms (squares) and 4 s (triangles). The y-axis represents the probability of measuring the state $|\uparrow\rangle$. The number of measurements per phase point is 1000 and 100 for the 4 ms and 4 s phase scans, respectively. The contrast b for the 4 ms data is 0.933 ± 0.014 and for the 4 s data is 0.742 ± 0.043. The $\phi_D \simeq 1$ rad phase shift in the 4 ms data is due to detuning the local oscillator by the differential Stark shift (∼4.2 kHz) such that the Ramsey $\pi/2$-pulses are resonant. **(b)** Contrast vs. Ramsey interval T_R. Each datum represents the fitted contrast b for a phase scan with Ramsey interval T_R. The solid curve is a weighted least-squares fit to the data.

Before each experiment we perform Doppler cooling, resolved-sideband cooling, and optical pumping to bring the two ions to the vibrational ground state in the trap with internal state $|11\rangle$ [24]. As described in [25], we prepare the maximally entangled state

$$|\Phi_{-i}\rangle = \frac{1}{\sqrt{2}}(|00\rangle - i|11\rangle). \tag{5}$$

Following this step, we apply a rotation $R(\frac{\pi}{2}, -\frac{\pi}{4})$ to both ions to create the state, $|\Psi_+\rangle$.

After preparation of the $|\Psi_+\rangle$ state, we wait for a delay t_D and then apply a final rotation $R(\frac{\pi}{2}, 0)$ to both qubits. This transforms $|\Psi_+\rangle$ into the Bell state $|\Phi_+\rangle = \frac{1}{\sqrt{2}}(|00\rangle + |11\rangle)$, but does not affect the singlet state $|\Psi_-\rangle$ as it is invariant under collective rotations. We detect both ions simultaneously; from the fluorescence count distributions, we can determine the parity of the final state [26] and therefore the probabilities of $|\Psi_+\rangle$

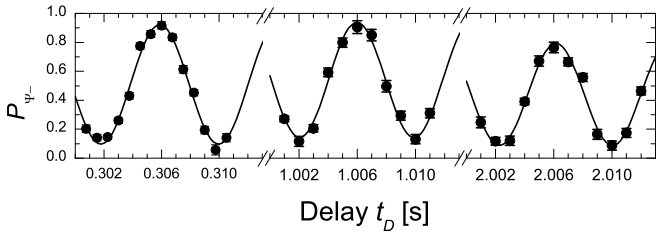

FIG. 4: Coherent oscillation between $|\Psi_+\rangle$ and $|\Psi_-\rangle$ states as a function of delay t_D. P_{Ψ_-} represents the probability of measuring $|\Psi_-\rangle$. The line is a sinusoidal fit to the data. Data are shown after delays of 300 ms, 1 s, and 2 s.

and $|\Psi_-\rangle$ in Eq. 4 as a function of t_D.

Figure 4 displays data for the coherent oscillation around three different delays t_D. For these data, the magnetic-field gradient induces an oscillation frequency of approximately 125 Hz. From the decay of the $|\Psi_+\rangle$, $|\Psi_-\rangle$ oscillations with delay t_D we extract a Bell-state lifetime of 7.3 ± 1.6 s, assuming exponential decay. The measured entanglement lifetime was limited by fluctuations in the magnetic-field gradient.

Combining field-independent qubits and DFS states, we could create memories even more robust than the DFS Bell states demonstrated here and in Ref. [23], as different local magnetic fields will induce very small frequency shifts of the qubit transition. The other two states in the Bell basis $\frac{1}{\sqrt{2}}(|00\rangle \pm |11\rangle)$ will also benefit from reduced decoherence due to magnetic field noise.

In summary, we have shown how field-independent qubits can serve as good memory elements in a trapped-ion-based quantum information processor. Decoherence-free-subspace (DFS) qubits as demonstrated here and in [6, 23] can also be used as good memory elements, with the additional overhead of encoding into the DFS states. Combining both techniques should lead to memory elements with extremely long coherence times. One disadvantage of field-independent qubits is that gates relying on differential Stark shifts between the qubit states [25] will cease to work when the qubit transition frequency is small compared to the Raman beam detuning from the excited states. To overcome this limitation, we can momentarily change the qubit states, perform the gate, and transform back to the original qubit basis. If the ambient magnetic fields fluctuate on time scales much longer than the duration of these three steps, accumulated phase errors should be negligible. Alternatively, we could apply a gate in which both bits are simultaneously flipped [27, 28, 29].

The demonstration of robust qubit memories and long-lived entanglement in trapped atomic ion systems satisfies one of the requirements necessary for large scale quantum information processing. Assuming exponential decay, the probability of memory error is 1.4×10^{-5} for current detection durations of 200 μs, which is below the fault-tolerant thresholds set by Steane [2] and Knill [30]. This, in combination with the ability to reduce spontaneous emission errors during laser excitation [31], makes atomic ion systems promising candidates for fault-tolerant QIP.

The authors thank Jeroen Koelemeij and Signe Seidelin for helpful comments on the manuscript. This work was supported by the US National Security Agency (NSA) and the Advanced Research and Development Activity (ARDA) under contract number MOD-7171.05. This manuscript is a publication of NIST and is not subject to U. S. copyright.

* Electronic address: clanger@boulder.nist.gov
† Present address: Department of Physics, University of Illinois at Urbana-Champaign, Urbana, IL 61801-3080
‡ Present address: Department of Physics, Technion - Israel Institute of Technology, Technion City, Haifa 32000, Israel
§ Present address: Max Planck Inst Quantum Opt, Hans Kopfermann Str 1, Garching, D-85748 Germany
¶ Present address: Institute for Experimental Physics, University of Innsbruck Technikerstr. 25, 5020 Innsbruck, Austria

[1] J. Preskill, Proc. R. Soc. Lond. A **454**, 385 (1998).
[2] A. M. Steane, Phys. Rev. A **68**, 042322 (2003).
[3] E. Knill, R. Laflamme, and W. H. Zurek, Proc. R. Soc. Lond. A **454**, 365 (1998).
[4] M. D. Barrett *et al.*, Nature **429**, 737 (2004).
[5] M. Riebe *et al.*, Nature **429**, 734 (2004).
[6] D. Kielpinski *et al.*, Science **291**, 1013 (2001).
[7] S. A. Diddams *et al.*, Science **306**, 1318 (2004).
[8] P. T. H. Fisk *et al.*, IEEE Trans. on Instrum. and Meas. **44**, 113 (1995).
[9] J. J. Bollinger *et al.*, IEEE Trans. on Instrum. and Meas. **40**, 126 (1991).
[10] D. M. Harber, H. J. Lewandowski, J. M. McGuirk, and E. A. Cornell, Phys. Rev. A **66**, 053616 (2002).
[11] P. Treutlein, P. Hommelhoff, T. Steinmetz, T. W. Hänsch, and J. Reichel, Phys. Rev. Lett. **92**, 203005 (2004).
[12] F. Mintert and C. Wunderlich, Phys. Rev. Lett. **87**, 257904 (2001).
[13] D. Schrader *et al.*, Phys. Rev. Lett. **93**, 150501 (2004).
[14] J. I. Cirac and P. Zoller, Phys. Rev. Lett. **74**, 4091 (1995).
[15] C. Monroe *et al.*, Phys. Rev. Lett. **75**, 4011 (1995).
[16] D. J. Wineland *et al.*, J. Res. Natl. Inst. Stand. Technol. **103** (3), 259 (1998).
[17] J. Chiaverini *et al.*, Nature **432**, 602 (2004).
[18] M. A. Rowe *et al.*, Quant. Inf. Comput. **2**, 257 (2002).
[19] P. J. Lee *et al.*, Opt. Lett. **28**, 1582 (2003).
[20] T. W. Hänsch and B. Couillaud, Opt. Comm. **35**, 441 (1980).
[21] N. F. Ramsey, Molecular Beams, Oxford University, London (1963).
[22] D. J. Wineland, J. J. Bollinger, and W. M. Itano, Phys. Rev. Lett. **50**, 628 (1983).
[23] C. F. Roos *et al.*, Phys. Rev. Lett. **92**, 220402 (2004).
[24] B. E. King *et al.*, Phys. Rev. Lett. **81**, 1525 (1998).

[25] D. Leibfried *et al.*, Nature **422**, 412, (2003).
[26] M. A. Rowe *et al.*, Nature **409**, 791 (2001).
[27] K. Mølmer and A. Sørensen, Phys. Rev. Lett. **82**, 1835 (1999).
[28] C. A. Sackett *et al.*, Nature **404**, 256 (2000).
[29] P. C. Haljan *et al.*, arXiv:quant-ph/0411068 (2004).
[30] E. Knill, Nature **434**, 39 (2005).
[31] R. Ozeri *et al.*, arXiv:quant-ph/0502063 (2005).